

# A Survey for Large Separation Lensed FIRST Quasars

Eran O. Ofek<sup>★1</sup>, Dan Maoz<sup>1</sup>, Francisco Prada<sup>2</sup>, Tsafrir Kolatt<sup>3</sup>, Hans-Walter Rix<sup>4</sup>

<sup>1</sup> School of Physics and Astronomy and Wise Observatory, Tel Aviv University, Tel Aviv 69978, Israel

<sup>2</sup> Centro Astronomico Hispano-Aleman, Apdo 511, E-04080 Almeria, Spain

<sup>3</sup> Racah Institute for Physics, The Hebrew University, Jerusalem 91904, Israel

<sup>4</sup> Max-Planck-Institut für Astronomie, Königstuhl 17, D-69117 Heidelberg, Germany

Accepted ? Received ? in original form ?

## ABSTRACT

Little is known about the statistics of gravitationally lensed quasars at large ( $7'' - 30''$ ) image separations, which probe masses on the scale of galaxy clusters. We have carried out a survey for gravitationally-lensed objects, among sources in the FIRST 20cm radio survey that have unresolved optical counterparts in the digitizations of the Palomar Observatory Sky Survey. From the statistics of ongoing surveys that search for quasars among FIRST sources, we estimate that there are about 9100 quasars in this source sample, making this one of the largest lensing surveys to date. Using broad-band imaging, we have isolated all objects with double radio components separated by  $5'' - 30''$ , that have unresolved optical counterparts with similar *BVI* colours. Our criteria for similar colours conservatively allow for observational error and for colour variations due to time delays between lensed images. Spectroscopy of these candidates shows that none of the pairs are lensed quasars. This sets an upper limit (95% confidence) on the lensing fraction in this survey of  $3.3 \times 10^{-4}$ , assuming 9100 quasars. Although the source redshift distribution is poorly known, a rough calculation of the expected lensing frequency and the detection efficiencies and biases suggests that simple theoretical expectations are of the same order of magnitude as our observational upper limit. Our procedure is novel in that our exhaustive search for lensed objects does not require prior identification of the quasars in the sample as such. Characterization of the FIRST-selected quasar population will enable using our result to constrain quantitatively the mass properties of clusters.

**Key words:** cosmology: gravitational lensing – galaxies: clusters: general – quasars: general

## 1 INTRODUCTION

The statistics of gravitational lensing can provide a powerful probe of the geometry and the mass content of the universe out to large redshifts (e.g. Refsdal 1964; Press & Gunn 1973). Turner, Ostriker, & Gott (1984) first explored lensing probabilities due to galaxies, and the resulting image separation distributions. The *Hubble Space Telescope (HST)* Snapshot Survey for lensed quasars (Bahcall et al. 1992; Maoz et al. 1992; 1993a; 1993b) was the first such large survey of a well-defined sample of 498 quasars. Exploiting the angular resolution of *HST*, it was shown that about 1% of luminous quasars at  $z > 1$  are gravitationally lensed into multiple images with separations in the  $0.''1 - 7''$  range. Maoz & Rix (1993) used the Snapshot Survey results to demonstrate

that early-type galaxies must have, on average, dark massive haloes similar to those of spiral galaxies, and that the geometry of the Universe is not dominated by a cosmological constant  $\Omega_\Lambda$ , setting an upper limit of  $\Omega_\Lambda < 0.7$ , with 95% confidence level (CL). Ground-based surveys of 360 additional quasars and their analysis (see Kochanek 1996, and references therein) have confirmed these results. Fukugita & Peebles (1993) and Malhotra, Rhoads, & Turner (1997) have suggested that small-separation lensing statistics can be reconciled with a  $\Omega_\Lambda$ -dominated Universe (as recently implied by high- $z$  Ia supernovae; Riess et al. 1998; Perlmutter et al. 1999) by invoking dust in the lensing galaxies. The excess number of lensed quasars would then be hidden by extinction (see, however, Falco et al. 1999). Recently, Chiba & Yoshii (1999) have recalculated the lensing statistics, by using revised values for the galaxy luminosity function parameters, and have argued that a universe with matter density  $\Omega_0 = 0.3_{-0.1}^{+0.2}$  and  $\Omega_0 + \Omega_\Lambda = 1$  is the most likely one.

<sup>★</sup> e-mail: eran@wise.tau.ac.il

While the statistics of gravitationally lensed quasars with multiple images in the angular range expected due to galaxy lensing have been probed by the Snapshot and other surveys, less is known about lensed-quasar statistics at larger image separations, which probe masses on the scale of galaxy clusters. Kochanek, Falco, & Schild (1995) have reported work in progress on a search out to 12'' separations, but most of the large separation candidates have yet to be rejected. Maoz et al. (1997, see below) found no large separation lenses among a small sample of 76 optically-selected quasars. The Jodrell Bank VLA Astrometric Survey (JVAS; King et al. 1996) and the Cosmic Lens All-Sky Survey (CLASS; Myers 1996) for lensing among flat-spectrum radio sources have the potential to uncover large numbers of lensed quasars. An extension of the JVAS survey, for gravitational lensing among  $\sim 2500$  flat spectrum sources in the 6''-60'' separation range, is reported preliminarily in Marlow et al. (1998). Phillips et al. (2000b) report a search in the 6'' to 15'' separation range of the combined JVAS/CLASS sample, with all but one of the  $\sim 15,000$  sources currently rejected as being gravitationally lensed. Shanks et al. (2000) discuss preliminary results for the first 6000 quasars from the 2dF survey, in which one large-separation candidate gravitational lens has been found. At present, there are no confirmed cases of quasar splittings with separations above 7''.

Recently, Phillips, Browne, & Wilkinson (2000a) have presented null results from a survey for large separation lensing which has several analogs to the survey we will describe in the present paper. They have searched for lensed objects among 1023 extended radio sources in the FIRST radio survey that are brighter than 35mJy, and that have point-like APM optical counterparts (See §2, below, for details and references for these radio and optical catalogs). Each such radio source was searched for radio companions brighter than 7mJy with separations in the range 15'' to 60''. Followup observations with the VLA and MERLIN shows that none of the 38 candidates is a gravitational lens system, based on a morphological distinction between lensed objects and physical multiple radio structures. The choice of studying only extended FIRST sources was meant to deal with the problem of variability and the long time delay (tens to hundreds of years) expected between images in large-separation lenses; significant changes cannot occur on such timescales in the shapes and fluxes of the physically-extended structures in the sample Phillips et al. (2000a) have defined.

As described in detail below, our lensing survey is limited to the 5'' to 30'' separation range, but uses all FIRST sources, both extended and unresolved, that have optical counterparts, and any or all of the multiple FIRST sources may be as faint as 1 mJy. Our sample is therefore considerably larger than Phillips et al.'s (2000a), and we show that it includes about 9100 quasars. As opposed to a morphological analysis in the radio band, our survey uses optical color criteria and spectroscopy to reject objects as lensed. We rely on the observed longterm color-variation properties of quasars to address the time delay problem. Our survey thus complements and extends the Phillips et al. (2000a) work. Their null result suggests that our study has not missed a large population of lensed quasars due to quasar color variability combined with large time delays. However, the comparison of the two studies is not straightforward, since their different selection criteria result in different source redshift distribu-

tions, detection limits for lensed pairs, and magnification biases.

The theoretically-expected statistics of large-separation lensing have been studied by Narayan & White (1988), Cen et al. (1994), Wambsganss et al. (1995), Kochanek (1995), Flores & Primack (1996), Maoz et al. (1997), Wyithe, Turner & Spergel (2000), Li & Ostriker (2000), and Keeton & Madau (2000). Maoz et al. (1997) presented the results of a preliminary survey for large-separation lensed quasars among known optically-selected quasars. They used multi-colour photometry and spectroscopy to show that none of the point sources in the entire  $70'' \times 70''$  field of view of the *HST* Planetary Camera exposures of 76 quasars in the original Snapshot Survey could be lensed images of the quasars. The 76 quasars were a selection that is unbiased against lensing out of the 498 Snapshot quasars, and their study demonstrated that large image-separation lensing is not common. Maoz et al. (1997) then carried out a calculation of the expected lensing statistics for that particular sample and its observational parameters. In addition to including effects such as magnification bias and observational detection limits, their calculation used a cluster mass profile that is motivated by N-body simulations (Navarro, Frenk, & White 1995a, 1995b, 1996, 1997; NFW) and observations (Carlberg et al. 1997; Bartelmann 1996). They found that, if  $\gamma$ , the power-law index relating the scale radius  $r_s$  to the total cluster mass in an NFW profile is large enough (e.g.  $\gamma = 1$ ), then low- and intermediate-mass clusters have a large central density, and can lens more efficiently than the singular and cored isothermal mass distributions that have been traditionally considered. Further study of the lensing effect of the NFW profile, and its generalizations, have been carried out by Wyithe, Turner & Spergel (2000), Li & Ostriker (2000), and Keeton & Madau (2000), the latter tailored particularly to the observational results of Phillips et al. (2000b).

There is thus a real possibility that large separation lenses can be found in a large enough sample, and their existence can then be used to learn about cluster mass-structure, number density, and redshift evolution. Alternatively, a null result can be used to constrain these quantities. The mass profile of clusters is closely related to the nature of the dark matter of which clusters are composed, while the number density and evolution are sensitive to the cosmological background parameters. These considerations can be used to obtain constraints on  $\Omega_\Lambda$ , similar to those derived from the statistics of small separation images. The dust extinction argument (e.g. Malhotra, Rhoads, & Turner 1997) is probably not applicable to lensing by clusters, since rich clusters do not significantly redden quasars that are behind them (Maoz 1995).

We have carried out a survey for large-separation lensed images using a very large extragalactic source database, the FIRST radio survey. In §2.1 we review the basic properties of the FIRST survey and the APM and USNO digitizations of the first epoch Palomar Observatory Sky Survey (POSS-I), and in §2.2 we describe how they were used to select candidate lensed sources. Our observations are described in §3, and we summarize the survey results in §4, where we also provide a rough comparison of our results to theoretical expectations. To interpret thoroughly the survey results we need to know the redshift distribution of the sources and their luminosity function, in addition to the observational

detection efficiencies. Since not all the statistical properties of the quasars in our sample are yet known, we postpone the full theoretical interpretation of our results to a future paper.

## 2 CANDIDATE SELECTION

A survey for strong lensing requires a large, systematically selected, high-redshift sample of point sources. The quasars in the FIRST radio survey constitute such a sample. As we show below, there are  $\sim 10^4$  quasars at redshift  $z \sim 1$  in the FIRST catalog. However, most of these are as of yet not identified. Our strategy is, therefore, to select from the FIRST catalog with the aid of the APM and USNO-A optical catalogs, all objects that could potentially be quasars that have been lensed into multiple images with large separations.

### 2.1 The FIRST Radio Catalog and its Quasar Content

FIRST, *Faint Images of the Radio Sky at Twenty-cm* (Becker, White & Helfand 1994, White et al. 1997) is a project designed to produce the radio equivalent of the POSS over  $10,000\text{deg}^2$  of the north and south Galactic caps. The survey utilizes the National Radio Astronomical Observatories (NRAO) Very Large Array (VLA) in the B configuration with bandwidth-synthesis mode and fourteen 3-MHz-wide channels centered at 1400 MHz (20 cm). This allows for a relatively small beam size ( $5.^{\prime\prime}4$  in the northern catalog and  $5.^{\prime\prime}4 \times 6.^{\prime\prime}4$  in the southern catalog) and hence good angular resolution and astrometric accuracy (90% confidence positional error circle better than  $1''$ ). The beam size enables the detection of source structure down to scales of  $\sim 2.^{\prime\prime}5$ . Comparisons between the FIRST catalog and standard radio calibration sources, indicates that the systematic astrometry errors are smaller than  $0.^{\prime\prime}2$  (Gregg et al. 1996). The typical root-mean-square (RMS) noise of 0.15 mJy allows  $5\sigma$  detection of 1 mJy sources.

For our work, we used the 1999, July 21, version of the FIRST catalog, including  $\sim 5400\text{deg}^2$ , above Galactic latitude  $+25^\circ$ , between declinations  $-5^\circ$  and  $+58^\circ$ . The catalog also covers two narrow strips in the southern Galactic cap centered near declinations  $0^\circ$  and  $-9^\circ$ , comprising an additional  $\sim 610\text{deg}^2$ . There are 549,707 sources in the entire catalog, of which 54,537 are in the southern catalog. Over 99.9% of the sources in the FIRST catalog are extragalactic (Helfand et al. 1999). Helfand et al. (1998b) estimate that the mean redshift of FIRST sources is  $z \sim 1$ .

The FIRST Bright QSO Survey (FBQS; Gregg et al. 1996; White et al. 2000), is a spectroscopic survey of all FIRST (1997, April 24 version,  $2682\text{deg}^2$ ) objects with optical counterparts within  $1.^{\prime\prime}2$  of the FIRST sources that are classified as stellar on either of the two emulsions,  $O$  (blue) or  $E$  (red) in the Automated Plate Machine (APM; McMahon, & Irwin 1992) scan of the POSS-I/UKST plates, that after correcting for Galactic extinction, are brighter than  $E_{APM} = 17.8$  mag, and have colour  $O - E < 2$  mag. The  $O$  and  $E$  passbands have effective wavelengths (widths) of roughly  $4200\text{\AA}$ ( $1200\text{\AA}$ ) and  $6400\text{\AA}$ , ( $400\text{\AA}$ ), respectively.

White et al. (2000) found that  $51.4\% \pm 2.0\%$  (Poisson errors) of FIRST sources passing their selection criteria are quasars. The preliminary FBQS sample described by Gregg et al. (1996), used a positional coincidence criterion of  $2.^{\prime\prime}0$  instead of  $1.^{\prime\prime}2$ , and no colour criterion. They showed that the more strict positional criterion would eliminate only about  $4.4\% \pm 2.5\%$  (Poisson error) of the FBQS quasars. However, the requirement of close positional coincidence excludes extended, lobe-dominated, radio sources with no core component. Although Gregg et al. (1996) did not find any red quasars with  $O - E \geq 2$  mag, the red colour cut used in the full FBQS sample may make the survey incomplete for high redshift or obscured quasars. The mean and median redshifts of FBQS quasars are 1.05 and 0.95, respectively.

Becker et al. (1998) described an extension to the FBQS, to a limiting magnitude of  $E_{APM} = 19.0$  mag, named the FIRST Faint Quasar Survey (FFQS). The other FFQS selection criteria are similar to those of the FBQS. The fraction of quasars in the FFQS is about 90%, almost all with  $z > 0.5$  (M. Brotherton, 1999 - private communication). The FFQS sample incompleteness may be greater due to the colour cut, since the fainter quasars may be at higher redshift and hence redder. However, the number of quasars missed in the FFQS because of the colour criterion is unknown. Helfand et al. (1998a) describe a search for optical counterparts to radio sources from the FIRST survey, using the deep  $16\text{deg}^2$   $I$ -band survey of Postman et al. (1997) to a limiting magnitude  $I \sim 24$ . They detect 700 out of 1131 FIRST sources in this field. Spectroscopic identifications have been obtained for a significant fraction of the stellar counterparts. Most, as expected, are quasars.

An independent digitization of the POSS-I and UKST plates is the USNO catalog (Monet et al. 1997), which covers the entire sky. It includes all sources that have positional coincidence to within  $2''$  on both the  $E$  and  $O$  plates (in the northern hemisphere), or the  $SRC - J$  and  $ESO - R$  plates (in the southern hemisphere) of the POSS-I/UKST.

Our survey for large separation lensed quasars utilizes both the APM and the USNO-A1.0 catalogs to produce two candidate lensed quasar samples, as described in details below. In order to relate these two digitizations of the POSS-I, we compared the photometry of the USNO-A catalog, the APM photometry, and calibrated Johnson-Cousins  $B$  and  $R$  photometry of stars in random fields measured at Wise Observatory. The mean scatter in the USNO-A1.0 photometry is 0.38 mag in the  $E$  band, and 0.36 mag in the  $O$  band. In some magnitude ranges the USNO magnitudes also have systematic offsets of  $\pm 0.3$  mag. For the APM catalog we find a smaller scatter of up to 0.2 mag and systematic errors of up to 0.7 mag. The APM  $E = 17.8$  mag limit in the FBQS corresponds to  $E \approx 18.0$  in the USNO-A1.0 magnitude system and it is equivalent to  $R \approx 17.8$  mag in the Cousins  $R$  band. The  $E = 19.0$  mag limit of the FFQS corresponds to  $E \approx 19.0$  mag in the USNO-A1.0 magnitude system and to  $R \approx 19.0$  mag in the Cousins system. Caretta et al. (2000) compared the APM catalog with several others deep surveys, among them the ESO Imaging Survey (Nonino et al. 1999). They found that the APM is  $\sim 100\%$  complete to  $O_{APM} = 19.5$  mag, and  $\sim 70\%$  complete to  $O_{APM} = 21.5$  mag.

## 2.2 Source Samples and Selection of Lensed Candidates

We create a large extragalactic source sample, which we survey for large-separation lensed quasars, by correlating the FIRST catalog with the APM and USNO-A1.0 catalogs, as described below. The APM catalog covers about 96% of the area covered by the FIRST catalog, while the USNO-A1.0 catalog covers the entire sky. To produce our candidate lensed quasars for the FIRST-APM sample, we searched for APM optical counterparts within  $2.^{\circ}5$  of all FIRST sources<sup>†</sup>. We found 86,800 optical counterparts within  $2.^{\circ}5$ , and 64,154 optical counterparts within  $1.^{\circ}2$ , of the radio position. Although the FIRST 90%-confidence error radius is less than  $1''$ , we chose the large threshold to ensure that we do not miss any optical counterparts. Furthermore, some of the quasars could have extended radio structure that is not completely coincident with the optical source. While this large threshold increases the number of candidate lenses that need to be tested by subsequent observations, it does not adversely affect the statistics of the survey.

Following the FBQS selection criteria, we isolated all the pairs of radio-optical sources having separations of  $5''$  to  $30''$ , in which both pair members are point-like in at least one of the POSS/UKST  $O$  or  $E$  plates and in which both members have  $O - E < 2$  mag. As in the FBQS, before implementing the colour and magnitude criteria, we applied an extinction correction to each object using the  $E(B - V)$  map of Schlegel, Finkbeiner, & Davis (1998),  $A(E) = 2.7E(B - V)$  and  $A(O) = 4.4E(B - V)$ . These corrections are usually quite small. The median values for our source list is  $A(E) = 0.068$  mag and  $A(O) = 0.111$  mag.

In order to estimate the number of quasars in the FIRST-APM sample, we have counted the number of FIRST optical counterparts in the APM catalog satisfying the FBQS/FFQS criteria (point-like in at least one of the plates,  $O - E < 2$  mag, and up to  $1.^{\circ}2$  positional coincidence), as a function of magnitude. We found 2155 optical counterparts brighter than  $E_{APM} = 17.8$  mag and 8300 optical counterparts fainter than  $E_{APM} = 17.8$  mag, or a total of 10,455 objects with up to  $1.^{\circ}2$  positional coincidence (or 12,576 objects with up to  $2.^{\circ}5$  positional coincidence). We fit a second order polynomial to the observed fraction of quasars among FBQS candidates, as a function of magnitude, given in Figure 4 of White et al. (2000). Between  $E_{APM} = 18$  and 19 mag, the fit is constrained to a fraction of 90%, in accordance with the preliminary FFQS results (M. Brotherton, 1999 - private communication). Among optical counterparts fainter than  $E_{APM} = 19$  mag, we assumed the same quasar fraction fraction as in the FFQS. Our adopted fraction of quasars ( $F_{qso}$ ) as function of  $E$  magnitude is:

$$F_{qso} = \begin{cases} -0.9389 + 0.046E + 0.0027E^2, & E < 18 \\ 0.9, & E \geq 18 \end{cases} \quad (1)$$

The number of quasars in our sample is given by integrating, over magnitude, the fraction of quasars multiplied by the number of candidates,  $N_{cand}(E)$ , as a function of magnitude:  $\int F_{qso}(E)N_{cand}(E)dE \cong 8900$ . As mentioned above,

<sup>†</sup> The catalog of APM optical counterparts is available from: <http://wise-obs.tau.ac.il/~eran/SLSL/>

Gregg et al. (1996) found that about 4% of the optical counterparts with a radio-optical positional coincidence in the range  $1.^{\circ}2$  to  $2.^{\circ}0$  are quasars, adding another  $\sim 200$  quasars to our sample. Thus the number of quasars in our sample, of the type being found by the FBQS and FFQS, is about  $9100^{+500}_{-4000}$ , where the bounds are obtained by assuming the fraction of quasars among objects fainter than  $E_{APM} = 19$  mag is 0 or 1. However, from the preliminary results of Helfand et al. (1998a), it is unlikely that the number of quasars in our survey is near the lower bound (e.g. 5100). A more accurate estimate of the number of quasars in the survey and their properties must await the full results of the FFQS and the optical identifications of radio sources in the Postman et al. (1997) field. We are also exploring the use of the Sloan Digital Sky Survey (SDSS) to obtain a better estimate of the faint quasars fraction.

The procedure described above could potentially exclude some FIRST quasars from our source list. The colour criterion used in the FBQS and FFQS could exclude a population of red quasars (e.g., quasars with  $z \gtrsim 2.5$ , or highly obscured quasars). Based on the preliminary FBQS (Gregg et al. 1996), the fraction of missed red quasars is probably small in the FBQS ( $< 4.3\%$  with 95% CL; from Poisson statistics), but possibly larger in the FFQS. Some FIRST quasars could also be missed if the APM catalog misclassified some point-like sources as galaxies. However, this is less likely since Caretta et al. (2000) found that the fraction of point-like objects that were misclassified as galaxies by the APM is smaller than 3%, up to  $O \sim 20.5$ . Finally, either of the two POSS digitizations, the APM and the USNO catalogs, could be incomplete.

To investigate for the possible signatures of these effects, we created a second source sample by cross-correlating an earlier (i.e., smaller) version of the FIRST catalog (1998, February 4th;  $4760^{\circ}$ ) with the USNO-A1.0 catalog. In creating this sample, we ignored the POSS colour information, i.e., we included both blue and red objects. We also did not rely on the morphological classification of the APM (contrary to the APM, the USNO catalog does not provide morphological information), but rather accepted objects as point-like only based on our own subsequent CCD images. Thus, this sample may be considered a conservative sub-sample, intended to test for the potential problems outlined above. For each pair of FIRST radio sources we used a modified version of the REFNET<sup>‡</sup> program to search the USNO-A1.0 catalog for optical counterparts to both members of the radio pair within  $2.^{\circ}5$ .

Comparing the source lists produced with the APM and the USNO catalogs when the same criteria are applied to both (i.e., no morphological or colour criteria), we find that the APM list includes  $\sim 90\%$  of USNO sources, and the USNO-A1.0 catalog includes a similar fraction of APM sources. A check of the missing sources in both catalogs, shows that they are extended galaxies, or in few cases, bright stars ( $E \lesssim 12$  mag) for which the source centering by USNO-A1.0 and APM is different. We conclude that this test does not reveal evidence for incompleteness in either catalogs.

<sup>‡</sup> The original Astronomical REference NETwork program was written by Ted Bowell & Bruce Koehn, Lowell Observatory. [ftp://ftp.lowell.edu/pub/koehn/starnet/dist.html](http://ftp.lowell.edu/pub/koehn/starnet/dist.html)

The APM sample selection process produced 9 pairs (7 in the north and 2 in the south) having up to  $30''$  separation between pair members, while the USNO sub-sample selection process produced 226 pairs (209 in the north, 16 in the south). There is overlap between these two samples, such that there is a total of 230 actual pairs. In about 20% of these pairs, at least one of the members is listed as a galaxy in the NED<sup>§</sup> archive and was therefore eliminated as a lensed quasar. In principle, the two-band POSS photometry (either APM or USNO) and the FIRST 20 cm flux could have been used to reject as lensed those objects having different flux ratios in different bands. However, as shown in §2.1, the POSS magnitudes have a large error of  $\sim 0.2/0.4$  mag (for the APM and USNO-A1.0 respectively). Furthermore, the time delay expected between images in the case of large separation lenses can be of order of years to centuries, and we lack any knowledge on the variability of the optical-to-radio ratio on such large time-scales. We therefore ignored the FIRST and POSS flux/magnitude information when compiling our candidate lists.

In summary, we have defined from the FIRST catalog a sample of sources with the following properties: All radio sources brighter than 1mJy with point-like APM optical counterparts ( $\sim 70\%$  complete to  $O_{APM} = 21.5$  mag) that are bluer than  $O - E = 2$  mag. In a second sample used mainly for completeness checks, we used the USNO-A1.0 catalog and a FIRST sub-sample, this time with no colour or morphology criteria. From both samples we have isolated all pairs with  $\leq 30''$  separation, which constitute a sample of candidate lensed quasars.

### 3 OBSERVATIONS

In order to proceed we carried out broad-band photometry and/or spectroscopy for all pairs in the two samples that are not listed as galaxies in the NED archive. Using the Wise Observatory 1.0m telescope with a back-illuminated Tektronix 1024  $\times$  1024 CCD, on 50 nights between 1998, April and 1999, July, we acquired  $I$ ,  $V$  and  $B$  images for 178 pairs. Some  $R$ -band images of the pairs were kindly obtained by R. Uglesich in 1999, January with the MDM 1.4m telescope using the Echelle 2048  $\times$  2048 CCD.

The images were reduced in the standard way, using the IRAF<sup>¶</sup> package. We programmed a task<sup>||</sup> to identify the sources automatically by finding the astrometric solution of each image. The optical and radio positions for the pair were then marked on the image for visual inspection, and the optical source coincident with the radio source was measured using the APPHOT task. Sources that were resolved in any of the bands were rejected as lensed quasars. About 84% of the pairs were rejected based on this criterion. Although resolved galaxies undergo strong lensing with large image separations, in that case they are always distorted

<sup>§</sup> NASA-IPAC Extragalactic Database, <http://nedwww.ipac.caltech.edu/>

<sup>¶</sup> Image Reduction and Analysis Facility - is written and supported at the National Optical Astronomy Observatories (NOAO)

<sup>||</sup> Available from <http://wise-obs.tau.ac.il/~eran/iraf/>

into arcs. Our point source criterion might however, accidentally exclude multiply-imaged quasars in which one or more nearly-merging image pairs appear as one, marginally-resolved object, and this will need to be accounted for in the theoretical interpretation of our results.

Next, we measured the flux ratios in each band, and compared them. Since gravitational lensing is achromatic, pairs with different flux ratios (see below) were rejected as being lensed quasars. A possible problem with the flux-ratio comparison is the time delay between lensed images. For cluster lenses, this delay can be of order years to centuries. Giveon et al. (1999) monitored 42 (35 radio-quiet and 7 radio-loud) quasars for 7 years in the  $B$  and  $R$  bands, and found that the  $1\sigma$   $B - R$  variability in their sample was 0.053 mag. In order to minimize false rejections, we allowed for such variability when calculating the flux ratios of pairs. It is possible that on time-scales longer than  $\sim 7$  years, but which are still relevant to large separation lensing, larger colour changes occur in quasars. If so, our flux-based rejection criterion (and even spectroscopic criteria) may eliminate true lensed pairs. However, Helfand et al. (2000) recently examined the  $B$  and  $R$  variations of FIRST quasars over  $\sim 50$  yr timescales, by comparing CCD photometry to the APM plate-based magnitudes. Their results suggest a small typical color change, comparable to that measured by Giveon et al. (1999), over these longer timescales. Nevertheless, the possibility of color changes needs to be tested by future studies of quasar variability, and by studying actual large-separation systems when such are found.

In each band, we calculated the magnitude difference, and its error, between the pair of sources. The magnitude differences in the three bands were compared in units of the standard error, and we rejected as possible lensing candidates the pairs for which the flux ratio in one or more of the optical bands differs by more than  $3.5\sigma$ :

$$|\Delta m_i - \Delta m_j| > 3.5\sqrt{\delta^2(\Delta m_i) + \delta^2(\Delta m_j) + 0.053^2}, \quad (2)$$

where  $\Delta m_i$  is the magnitude difference between a pair of objects in the  $i$ -th filter,  $\delta(\Delta m_i)$  is the error in the magnitude difference between a pair of objects in the  $i$ -th filter, and 0.053 mag is the allowed  $1\sigma$  colour variability. Following this analysis, 15 of the pairs from the two samples remained candidate lenses. Table 1<sup>\*\*</sup> lists the candidates with their coordinates, approximate APM optical magnitude, and radio flux. If available, for each candidate the optical magnitude differences and the largest colour difference (including the  $B - R \approx 0.053$  mag variability) in units of  $\sigma$ , are listed.

We obtained spectra for all the lensed candidates in 1999, May 17, and 2000, March 6, 7 and 8. The spectra were obtained using the TWIN double-channel spectrograph on the Calar-Alto 3.5m telescope, with the T07 & T13 grating and the 5500Å dichroic, covering the red channel with  $3.3 \text{ \AA pixel}^{-1}$  dispersion, and the blue channel with  $4.3 \text{ \AA pixel}^{-1}$  dispersion, respectively. The  $1.^{\prime\prime}8 \times 240''$

<sup>\*\*</sup> The full information for all the observed pairs can be found at <http://wise-obs.tau.ac.il/~eran/SLSL/>.

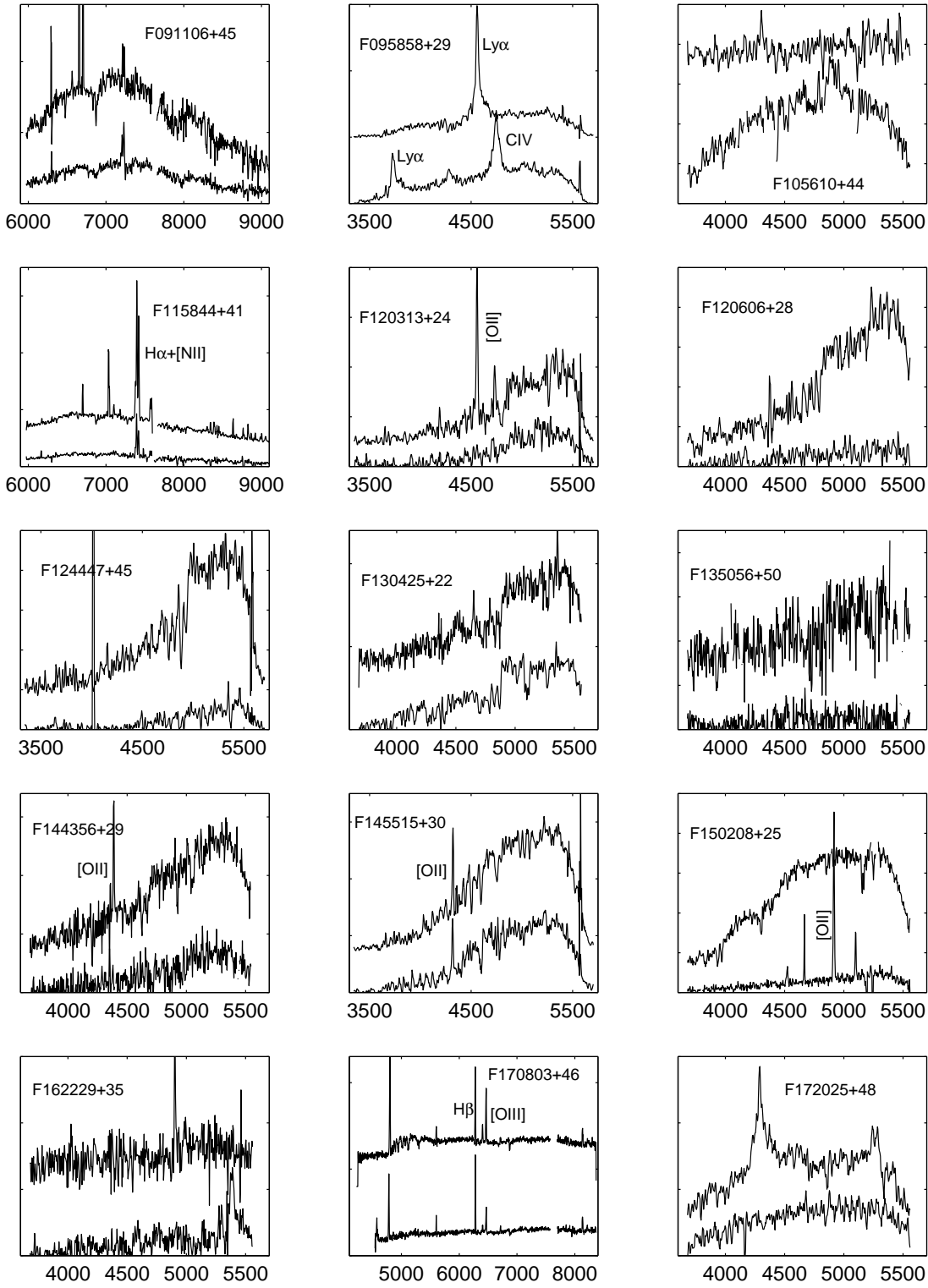


**Figure 1.** Spectra of candidate pairs. Vertical axis is counts in arbitrary units and horizontal axis is wavelength in Å. Additive shifts have been applied to some of the spectra for display purposes. Spectral regions with strong telluric absorption have been excluded. All spectra are from the Calar-Alto 3.5m telescope, except for F170803+46, which is from the Keck-II 10m telescope.

spectrograph slit was rotated to allow simultaneous observations of both members of each object pair. The spectra for additional pair was obtained on 1998, August 15, using the Keck-II 10m telescope with the LRIS spectrograph and

2.45 Å pixel<sup>-1</sup> dispersion. Figure 1 presents the spectra of the candidates.

The pairs are clearly ruled out as lensed quasars. All are either physical pairs of galaxies at  $z \sim 0.2$ , with velocity differences of order of 200 km s<sup>-1</sup>, or pairs of unrelated galax-

**Table 1.** Lensed Quasar Candidates

PLEASE PLACE TABLE 1 HERE

ies and quasars at different redshifts. Interestingly, our selection process, combined with the apparent rarity of large-separation lensing, seems to be successful at picking up physical pairs (possibly belonging to poor groups) of  $z \sim 0.1 - 0.3$  radio galaxies.

#### 4 DISCUSSION

We have surveyed a sample of about 9100 radio-selected quasars for large separation lensing. This is one of the largest surveys of its kind. The survey utilized the FIRST catalog in the radio, and the APM and USNO-A1.0 catalogs in the optical. Our observations show that none of the candidates turned up by our selection process is a gravitationally lensed quasar. Assuming the number of quasars in our FIRST-APM sample is 9100, this sets the probability for lensing in our sample at  $< 3.3 \times 10^{-4}$  with 95% CL (assuming Poisson statistics). This is an improvement of two-orders of magnitude over the large-separation lensing survey of Maoz et al. (1997). Our observations have identified several chance superposition of quasars and radio galaxies and several physical pairs of radio galaxies. We found no evidence for a missed population of red or misclassified quasars due to the FBQS, FFQS, or APM selection criteria, a population that could have been detected in the FIRST-USNO sample.

Our well defined statistical sample can be used to constrain the density profiles and mass function of galaxy clusters and to set limits on  $\Omega_\Lambda$  (e.g., Maoz et al. 1997). Although large-separation lensing probabilities have been calculated in the past (e.g., Flores & Primack 1996; Maoz et al. 1997, and reference therein), a detailed interpretation of the results reported here requires good knowledge of (1) the joint radio-optical luminosity function, to quantify magnification bias and (2) the redshift distribution of the quasars in our sample, to quantify the probed pathlength. We therefore must defer the full calculation of the theoretically expected lensing probability until completion of the FFQS and the spectroscopic identification of FIRST sources in the Postman et al. (1997) field.

However, a rough estimate of the optical depth, and hence the expected lensing frequency, can be obtained under various simplifying assumptions: We approximated the mass distributions of clusters as singular isothermal spheres (SIS), and then, following Turner et al. (1984), calculated the effective dimensionless density of lenses,  $F = 16\pi^3 n_0 \left(\frac{c}{H_0}\right)^3 \left(\frac{\sigma_{\parallel}}{c}\right)^4$ , where  $c$  is the speed of light,  $H_0$  the Hubble constant,  $\sigma_{\parallel}$  the line-of-sight velocity dispersion, and  $n_0$  the density of lenses. We assumed the observed Girardi et al. (1998) mass function for clusters and related the cluster mass,  $M$ , within  $r = 1.5h_{100}^{-1}$  Mpc (as defined by Girardi et al. 1998) to the line-of-sight velocity dispersion by  $\sigma_{\parallel}^2 = \frac{GM(< r)}{2r}$ , giving  $F = 0.0156^{+0.0118}_{-0.0067}$ . The errors in  $F$  were obtained from Monte-Carlo simulations using the

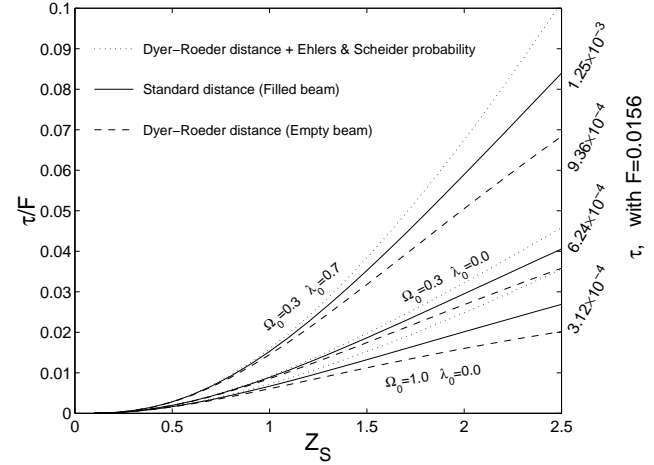


**Figure 2.** Weighted total optical depth for lensing by SIS clusters with the Girardi et al. (1998) mass function as a function of the source redshift. Three cosmological models are labeled, with three different distance/probability estimators for each model.  $F$  is the density of SIS lenses as defined by Turner et al. (1984).

errors in the Girardi et al. (1998) mass function parameters  $n^* = 2.6^{+0.5}_{-0.4} \times 10^{-5} (h_{100}^{-1} \text{ Mpc})^{-3} (10^{14} h_{100}^{-1} M_\odot)^{-1}$ , and  $M^* = 2.6^{+0.8}_{-0.6} \times 10^{14} h_{100}^{-1} M_\odot$ . For simplicity, we assumed that the errors in  $n^*$  and  $M^*$  are independent and normally distributed.

Figure 2 presents the SIS results for three cosmological models:  $\Omega_0 = 0.3$ ,  $\Omega_\Lambda = 0.7$ ;  $\Omega_0 = 0.3$ ,  $\Omega_\Lambda = 0.0$ ; and  $\Omega_0 = 1.0$ ,  $\Omega_\Lambda = 0.0$ . For each model we calculated the optical depth with the standard distance formula (solid line), the Dyer-Roeder distance formula (Dyer & Roeder 1972; 1973; broken line) and the Dyer-Roeder distance formula with the Ehlers and Schneider probability (1986; dotted line). For a median redshift of the FIRST quasars ( $z \sim 1$ ) the optical depth is about  $(0.5 - 4.4) \times 10^{-4}$ . To this range, a factor of 3.1 is contributed by the uncertainty in the mass function, and a factor of 2.3 is contributed by the uncertainty in the cosmology.

For an estimate of the lensing frequency, the optical depth to lensing needs to be multiplied by the following factors: (i) The detection efficiency due to the limited range of searched separations; (ii) The detection efficiency due to the survey's double-flux limit and the expected flux-ratio distribution; (iii) The magnification bias - the degree to which, at a given magnitude, lensed quasars are over/under-represented.

As described above, we searched for lensed quasars in the  $5''$  to  $30''$  separation range. Since we do not yet know the redshift distribution of FIRST quasars, we cannot calculate the exact image separation distribution expected from SIS lenses. However, assuming the typical ratio between the lens-source distance and observer-source distance is  $D_{ls}/D_{os} =$

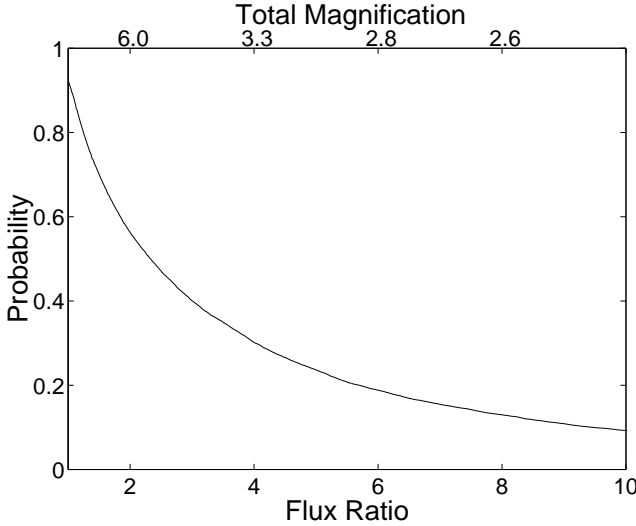


**Figure 3.** The probability that a lensed image of a quasar will pass the double ( $O$  and 20cm bands) detection limit of our survey, as a function of the flux ratio between the two images, or equivalently, as a function of the total magnification of a SIS lens.

1/2, the fraction of lenses with separations of  $5''$  to  $30''$  is 66%.

We have searched for lensed systems in a doubly (radio and optical) flux-limited sample. Since most objects are near the detection limit, the fainter member of the pair is often below the detection limit. In order to estimate this effect, we calculated the probability that a lensed image of a quasar will pass the double detection limits of our survey in the  $O$  and 20cm bands, as a function of the flux ratio between the two images. This was done as follows. From among all the optical counterparts with  $O - E < 2$  found within  $1.^{\circ}2$  from a radio source, we chose at random a list of "quasars", using Equation 1 for the fraction of quasars as function of magnitude. For each object in the list, the maximum observable flux ratio was found, using its optical magnitude and radio flux. The maximum observable flux ratio is defined as the flux ratio that a hypothetical fainter lensed image would have, and still be detected in both optical and radio bands. The flux ratio probability was then calculated. Until detailed information about the FIRST radio flux limit is available, we assumed it to be a step function at 1mJy. For the APM  $O$ -band detection limit, we adopted the APM completeness given by Caretta et al. (2000). Since 98% of the objects in our APM sample are brighter in  $E$  than in  $O$  (i.e.  $O - E > 0$ ), and the  $E$ -band completeness is similar to that of the  $O$ -band, we ignored the  $E$ -band completeness. This procedure assumes that the correlation between the radio flux and optical magnitude is negligible (as shown below), and that the flux ratio between the  $O$  band and the radio is the same for both images (i.e. neglecting variability). Figure 3 shows the result of this calculation.

Next, we considered the flux ratio distribution predicted by the lens model. The flux ratio between the two images in a SIS lens is  $R = \frac{1+\beta}{1-\beta}$  and the probability of an impact parameter  $\beta$  is  $dP = 2\beta d\beta$ . The flux ratio probability is  $dP = 4\frac{R-1}{(R+1)^3}dR$ . Figure 4 shows the probability density as function of the flux ratio resulting from the product of the

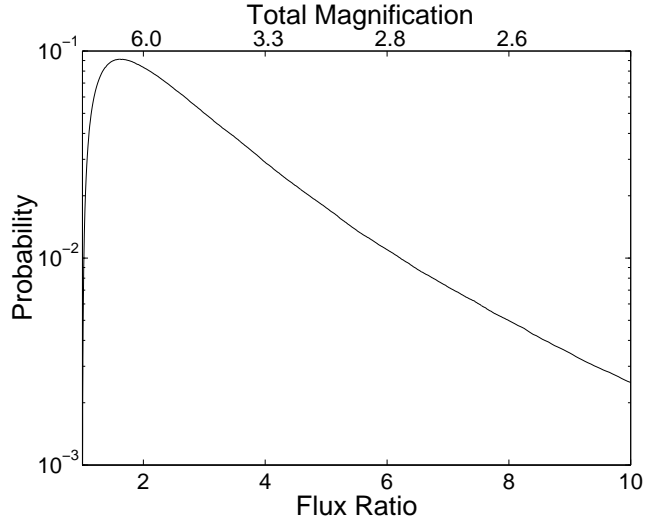


**Figure 4.** The probability density for finding a doubly-imaged lensed quasar with a given flux ratio, calculated by multiplying the flux ratio distribution of a SIS lens by the double flux limit selection function of the survey. The total magnification of a SIS lens is plotted in the upper axis for reference.

intrinsic flux ratio distribution due to the lens model and the flux ratio selection function (described above).

Following Turner et al. (1984), the magnification bias is given by,

$$B = \frac{\int_0^\infty \int_{A_M}^\infty A^{-1} P_I(A) P_D(A) N_Q(f/A) dA df}{\int_0^\infty N_Q(f) df}, \quad (3)$$

where  $f$  is the flux,  $A_M$  is the minimum amplification of the bright image (see Mortlock & Webster 2000) for a multiply imaged source (e.g. 2 for a SIS lens),  $P_I(A)$  is the intrinsic probability density for the amplification  $A$  of the brightest image due to the lens model,  $P_D(A)$  is the detection probability for the amplification  $A$  of the brightest image due to the flux ratio detection efficiency of the survey, and  $N_Q(f)$  is the number of quasars with unlensed flux  $f$ . Borgeest, Linde, & Refsdal (1991) showed that if there is a negligible correlation between the optical and radio fluxes of the objects, the double optical-radio magnification bias depends on the sum of the slopes of the radio and optical differential number counts. In our case the correlation is  $\sim 4\%$  with  $\sim 10^4$  degrees of freedom. Figure 5 shows the binned number counts for our sample's quasars in the  $O_{APM}$  band. Figure 6 shows the same for the 20cm band. To account for the quasar fraction, as measured in the FBQS and FFQS, in each magnitude bin a fraction  $F_{qso}(E)$  (as given by Equation 1) of objects was randomly chosen. The optical and radio slopes of the differential number counts are  $\alpha_{opt} = -1.65 \pm 0.04$  with  $\chi^2_{dof} = 1.17$ , and  $\alpha_{20cm} = -1.40 \pm 0.01$  with  $\chi^2_{dof} = 1.59$ , respectively. The total slope is  $-3.05 \pm 0.04$ . For a slope of  $-3$ , or smaller, the magnification bias integral diverges. In reality, however, there are probably breaks in the number count relations. The detection of such breaks is critical for the exact assessment of the magnification bias. We plan to address this problem by deriving the number-magnitude relations of similar, but smaller, radio-optical samples of objects. Such samples could be constructed from deeper opti-

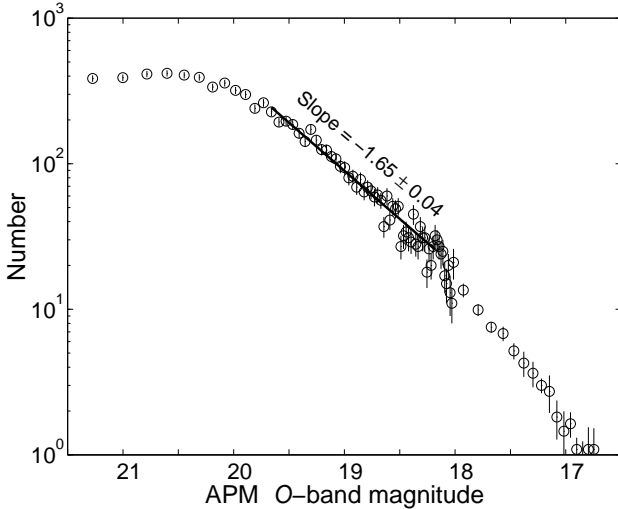


**Figure 5.** Differential number counts for our sample quasars in the  $O$  band. To account for the quasar fraction, as measured in the FBQS and FFQS, in each magnitude bin a fraction  $F_{qso}(E)$  (as given by Equation 1) of objects was randomly chosen. A power-law is fit to the data in the range  $O_{APM} < 19.75$  mag (100% completeness; Caretta et al. 2000) and  $O_{APM} > 18.25$  mag, where a change of slope is apparent. The slope  $-1.65 \pm 0.04$ , corresponds to 0.66 in the log  $N$ -mag plane. The points for objects brighter than 18 mag are the means of 10 adjoining bins.

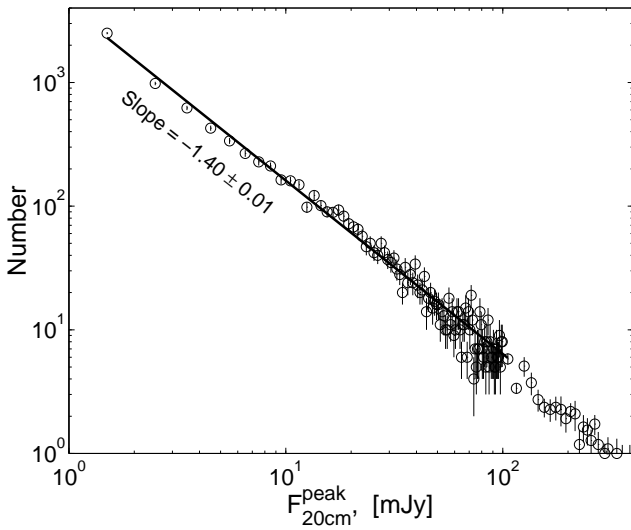


**Figure 6.** Same as Figure 5, but for the 20cm band.

cal (e.g. SDSS) and 21cm radio surveys (e.g. the PHOENIX Deep Survey, Hopkins et al. 1998; the ISO ELAIS Survey, Ciliegi et al. 1998).

Meanwhile, in order to obtain a rough estimate of the possible effect of the magnification bias, we assumed that below a flux  $f_{break}$ , the combined number counts slope changes from  $\alpha = -3.05$  to  $\alpha_{faint}$ , and we calculated the magnification bias as function of  $f_{break}/f_{limit}$ , for various values of  $\alpha_{faint}$ , where  $f_{limit}$  is the survey flux limit. Figure 7 presents the results for  $\alpha_{faint} = 1$  (solid line) and  $-2$  (dashed line). The gray area represents the  $1\sigma$  error for the solid-line (i.e.,  $\alpha$  changes from  $-3.09$  to  $1$  and from  $-3.01$  to  $1$ ). Based on

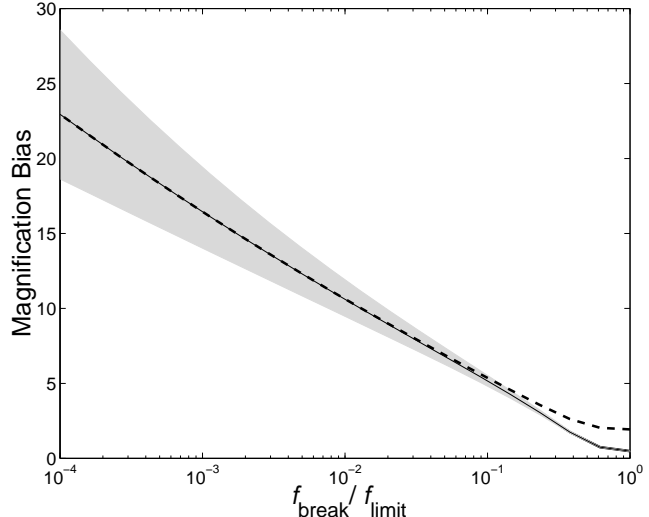


**Figure 7.** The magnification bias as a function of  $f_{break}/f_{limit}$ , for  $\alpha_{faint} = 1$  (solid line) and  $-2$  (dashed line). The gray area represents the  $1\sigma$  error for the solid-line (i.e.,  $\alpha$  changes from  $-3.09$  to  $1$  and from  $-3.01$  to  $1$ ).

these results, for our present rough calculation we adopt a magnification bias in the range  $1 - 30$ .

From the effects considered, namely, the double magnification bias and the double flux limit, we find that for a non-evolving Girardi et al. (1988) mass function, the predicted fraction of lensed quasars in our survey is in the range of  $(0.5 - 4.4) \times 10^{-4} \times 0.66 \times (1 - 30) \approx (0.3 - 87) \times 10^{-4}$ . Interestingly, this is of the same order as the 95% observational upper limit of  $3.3 \times 10^{-4}$ , obtained above. However, a more thorough calculation needs to be done. Apart from the unknown properties of FIRST quasars, models other than SIS (e.g. the NFW model or its generalizations; Maoz et al. 1997; Wyithe et al. 2000) may predict a lensing fraction lower or higher by an order of magnitude. It is possible that, once the detailed properties of the quasars in our sample are known, such models will predict high rates for our survey. If so, our results may be able to rule out some of the cosmological and cluster-structure parameter space.

The FIRST catalog has many other potential lensing applications (e.g. Andernach et al. 1998; Helfand et al. 1998b; Lehar et al. 1999). Additional possibilities are: (1) to search for lensed galaxies using the FIRST morphological information; (2) to combine the FIRST catalog with the good angular resolution of the 2MASS survey in order to find candidates for small-separation gravitational lensing. We will explore these possibilities in future papers.

## ACKNOWLEDGMENTS

We thank M. Brotherton, A. Gal-Yam, and P. GuhaThakurta, for observations with the Keck-II telescope and R. Uglesich for observations with the MDM telescope. We also thank M. Brotherton for communicating the preliminary results of the FFQS prior to publication. We are grateful to the referee, L. Miller, for his useful comments. EO wishes to thank Orly Gnat for fruitful discussions. Astronomy at Wise Observatory is sup-

ported by grants from the Israel Science Foundation. This work is partly supported by grants from NASA and NSF at UCSC and HU (TsK). This research has made use of the NASA/IPAC Extragalactic Database (NED) which is operated by the Jet Propulsion Laboratory, California Institute of Technology, under contract with the National Aeronautics and Space Administration. This research has made use of the APM catalogue run by the Institute of Astronomy in Cambridge.

## REFERENCES

- Andernach, H., Gubanov, A. G. and Slee, O. B. 1998, Observational Cosmology with the New Radio Surveys, 107
- Bahcall, J.N., Maoz, D., Doxsey, R., Schneider, D.P., Bahcall, N.A., Lahav, O., Yanny, B. 1992, ApJ, 387, 56
- Bartelmann, M. 1996, A&A, 313, 697-702
- Becker, R.H., White, R.L., Helfand, D.J., 1994, in Astronomical Data Analysis Software and Systems III, ASP Conference Series, v. 61, eds. D. R. Crabtree, R. J. Hanisch, & J. Barnes, p. 165
- Becker, R.H., et al. 1998, Am. Astron. Soc. Meeting, 192, 11.01.
- Borgeest, U., von Linde, J. and Refsdal, S. 1991, A&A, 251, L35
- Bullock, J.S., Kolatt, T.S., Sigad, Y., Somerville, R.S., Kravtsov, A.V., Klypin, A.A., Primack, J.R., Dekel, A. 1999, astro-ph/9908159
- Caretta, C.A., Maia, M. A. G. & Willmer, C. N. A. 2000, AJ, 119, 524
- Carlberg, R.G. et al. 1997, ApJ, 485, L13
- Cen, R., Gott, J.R., Ostriker, J.P., Turner, E.L. 1994, ApJ, 423, 1
- Chiba, M., Yoshii, Y. 1999, ApJ, 510, 42
- Ciliegi, P. 1998, MNRAS, 302, 222
- Dyer, C.C., Roeder, R.C. 1972, ApJ, 174, L115
- Dyer, C.C., Roeder, R.C. 1973, ApJ, 180, L31
- Ehlers, J. & Schneider, P. 1986, A&A, 168, 57
- Falco, E.E., et al. 1999, ApJ, 523, 617
- Flores, R.A., Primack, J.R. 1996, ApJ, 457, L5
- Fukugita, M., Peebles, P.J.E. 1993, astro-ph/9305002
- Girardi, M., Borgani, S., Giuricin, G., Mardirossian, F., Mezzetti, M. 1998, ApJ, 506, 45
- Giveon, U., Maoz, D., Kaspi, S., Netzer, H., Smith, P.S., 1999, MNRAS, 306, 637
- Gregg, M.D., Becker, R.H., White, R.L., Helfand, D.J., McMahon, R.G., Hook, I.M., 1996, AJ, 112, 407
- Helfand, D.J., Yadigaroglu, I.A., Berger, R., Postman, M., White, R.L., Lauer, T.R., Oegerle, W.R., Becker, R.H. 1998a, AAS, 193.4002
- Helfand, D. J., Brown, S., Kamionkowski, M., Cress, C., Refregier, A., Becker, R. H. and White, R. L. 1998b, American Astronomical Society Meeting, 192, 5211
- Helfand, D.J., Schnee, S., Becker, R.H., White, R.L., McMahon, R.G. 1999, AJ, 117, 1568
- Helfand, D.J. et al. 2000, ApJ, submitted.
- Hopkins, A.M., Mobasher, B., Cram, L., Rowan-Robinson, M. 1998, MNRAS 296, 839
- Keeton, C.R., Madau, P. 2000, ApJ, submitted
- King, L. J., Browne, I. W. A. and Wilkinson, P. N. 1996, IAU Symp. 173: Astrophysical Applications of Gravitational Lensing, 173, 191
- Kochanek, C.S. 1995, ApJ 453, 545
- Kochanek, C.S. 1996, ApJ 466, 638
- Kochanek, C.S., Falco, E.E., Schild, R. 1995, ApJ, 452, 109
- Lehar, J., Buchalter, A., McMahon, R., Kochanek, C., Helfand, D., Becker, R., Muxlow, T. 1999, astro-ph/9908353
- Li, L.-X., Ostriker, J.P. 2000, astro-ph/0010432
- Malhotra, S., Rhoads, J.E., Turner, E.L. 1997, MNRAS, 288, 138
- Maoz, D. 1995, ApJ, 455, L115
- Maoz, D., Bahcall, J.N., Schneider, D.P., Doxsey, R., Bahcall, N.A., Lahav, O. Yanny, B. 1992, ApJ, 394, 51
- Maoz, D., Bahcall, J.N., Schneider, D.P., Doxsey, R., Bahcall, N.A., Lahav, O. Yanny, B. 1993a, ApJ, 402, 69
- Maoz, D., et al. 1993b, ApJ, 409, 28
- Maoz, D., Rix, H.-W. 1993, ApJ, 416, 425
- Maoz, D., Rix, H.-W., Gal-Yam, A., Gould, A. 1997, ApJ, 486, 75-84
- Marlow, D.R., McGuinness, A.D., Browne, I.W.A., Wilkinson, P.N., Helbig, P.J. 1998, in: Large Scale Structure: Tracks and Traces. pp.327-328. Proceedings of the 12th Potsdam Cosmology Workshop. Eds. V. Mueller, S. Gottloeber, J.P. Muecket, J. Wambsganss. World Scientific.
- McMahon, R. G. and Irwin, M. J. 1992, Digitised Optical Sky Surveys, 417
- Monet, D., et al. 1997 USNO-A1.0, (U.S. Naval Observatory, Washington DC).
- Mortlock, D.J., Webster, R.L. 2000, astro-ph/0008081
- Myers, S.T. 1996, in Astrophysical Applications of Gravitational Lensing, ed. C.S. Kochanek & J.N. Hewitt (Dordrecht: Kluwer), 317
- Narayan, R., White, S.D.M. 1988, MNRAS, 231, 97
- Navarro, J., Frenk, C.S., White, S.D.M. 1995a, MNRAS, 275, 720
- Navarro, J., Frenk, C.S., White, S.D.M. 1995b, MNRAS, 275, 56
- Navarro, J., Frenk, C.S., White, S.D.M. 1996, ApJ, 462, 563
- Navarro, J., Frenk, C.S., White, S.D.M. 1997, ApJ, 490, 493
- Nonino, M., et al. 1999, A&AS, 137, 51
- Perlmutter, S., et al. 1999, ApJ, 517, 565
- Phillips, P.M., Browne, W.A., Wilkinson, P.N. 2000a, accepted to MNRAS, astro-ph/0009366
- Phillips, P.M., Browne, I.W.A., Wilkinson, P.N., Jackson, N.J. 2000b, astro-ph/0011032
- Postman, M., Lauer, T., Oegerle, W., Szapudi, I., Hoessel, J. 1997, AAS, 191.1903
- Press, W.H., Gunn, J.E. 1973, ApJ, 185, 397
- Refsdal, S. 1964, MNRAS, 128, 307
- Riess, A.F. et al. 1998, AJ, 116, 1009
- Schlegel, D. J., Finkbeiner, D. P. and Davis, M. 1998, ApJ, 500, 525
- Shanks, T., Boyle, B.J., Croom, S.M., Loaring, N., Miller, L., Smith, R.J. 2000, Clustering at High Redshift, Marseille, June 1999, eds. A. Mazure, O. LeFevre, V. Lebrun - astro-ph/0003206, in press
- Turner, E.L., Ostriker, J.P., Gott III, R. 1984, ApJ, 284, 1
- Wambsganss, J., Cen, R., Ostriker, J.P., Turner, E.L. 1995, Science, 268, 274
- White, R.L., Becker, R.H., Helfand, D.J., Gregg, M.D. 1997, ApJ, 475, 479
- White, R. L., et al. 2000, ApJS, 126, 133
- Wyithe, J.S.B., Turner, E.L., Spergel, D.N. 2000, astro-ph/0007354

TABLE 1. Lensed Quasar Candidates

#	$\alpha$ J2000	$\delta$	$Sep$ ["]	$E$ [mag]	$O-E$ West Object [mag]	$F^{20cm}$ [mJy]	$E$ [mag]	$O-E$ East Object [mag]	$F^{20cm}$ [mJy]	$\Delta m_I$	$\Delta m_V$	$\Delta m_B$
1	09:11:06.65	+45:43:45.0	22.7	15.6	2.1	6.2	17.3	2.0	1.9	$-0.91 \pm 0.06$	$-0.88 \pm 0.09$	$-0.82 \pm 0.0$
2	09:58:58.57	+29:47:53.9	11.4	19.2 <sup>a</sup>	1.3	45.8	19.2	-0.1	138.3	$+0.35 \pm 0.16$	$+0.21 \pm 0.05$	$+0.54 \pm 0.0$
3	10:56:10.29	+44:27:16.7	24.5	19.2	0.3	49.5	19.0	0.7	55.0	...	...	...
4	11:58:44.66	+41:34:26.3	11.7	16.7	1.8	1.1	18.1	2.5	1.0	$-1.20 \pm 0.12$	$-1.07 \pm 0.11$	$-1.22 \pm 0.0$
5	12:03:13.79	+24:21:36.3	28.1	18.4 <sup>a</sup>	2.4	17.5	17.2	2.7	3.0	$+0.93 \pm 0.08$	$+0.82 \pm 0.07$	$+0.79 \pm 0.0$
6	12:06:06.02	+28:55:55.9	8.3	15.5 <sup>a</sup>	3.7	2.7	17.2	3.4	4.0	$+0.89 \pm 0.06$	$+0.83 \pm 0.09$	<sup>b</sup> ...
7	12:44:47.77	+31:39:12.0	11.6	17.1	3.1	7.9	17.3	4.0	7.2	$-0.24 \pm 0.07$	$-0.35 \pm 0.09$	$-0.68 \pm 0.0$
8	13:04:25.86	+22:38:22.6	28.2	16.5 <sup>a</sup>	3.7	3.4	17.6	2.6	1.6	$-0.85 \pm 0.04$	$-0.72 \pm 0.03$	$-0.89 \pm 0.0$
9	13:50:56.42	+50:53:03.6	18.5	19.0	2.7	6.6	17.2	4.4	2.6	$+2.30 \pm 0.35$	$+1.87 \pm 0.27$	$+0.62 \pm 0.0$
10	14:43:56.91	+29:19:16.2	12.6	17.8 <sup>a</sup>	3.1	3.4	16.3	2.9	14.4	$+0.50 \pm 0.07$	$+0.54 \pm 0.09$	$+0.51 \pm 0.0$
11	14:55:15.47	+30:57:04.4	14.8	17.2 <sup>a</sup>	2.1	4.2	18.2	1.7	1.4	$-0.43 \pm 0.10$	$-0.33 \pm 0.07$	$-0.40 \pm 0.0$
12	15:02:08.29	+25:28:44.9	15.9	16.7	1.4	4.1	17.4	2.7	47.1	$-1.74 \pm 0.09$	$-1.90 \pm 0.09$	$-2.36 \pm 0.0$
13	16:22:29.54	+35:31:09.1	25.7	19.8	1.7	1.7	19.9	1.7	218.4	...	...	...
14	17:08:03.27	+46:48:59.5	10.1	18.7	1.7	1.7	18.0	1.6	3.3	$+0.36 \pm 0.06$	$+0.39 \pm 0.08$	$+0.37 \pm 0.0$
15	17:20:25.47	+48:03:21.4	19.3	19.8	1.0	29.9	19.5	1.0	9.7	...	...	...

Notes to Table 1.

Double point source radio/optical objects with similar colours ( $< 3.5\sigma$ ). For each pair, the coordinates given in the table are for the western object, the APM  $E$  and  $O$  magnitudes, respectively.  $F^{20cm}$  is the integrated radio flux at 20 cm.  $\Delta m_i$  is the measured  $i$ -band magnitude difference for

1. ( $T, z$ ) is the type (Q-Quasar; G-Galaxy; ?-Unknown) and redshift of the objects.

<sup>a</sup> - The APM magnitude for at least one band is not known, and therefore the  $E$  and  $O$  magnitudes are taken from the USNO-A1.0 catalog. <sup>b</sup> - observe in the  $B$  band.

#### Notes on individual objects:

2 - A red spectrum (not shown) of the eastern object shows  $CIII]\lambda 1909$  emission at 7125Å.

3 - Unidentified narrow line at 4305Å present only in the western object, and unidentified broad emission feature at 4914Å present only in the eastern object.

5 - No lines are present in the spectrum of the eastern object.

6 - No emission lines, Ca  $H&K$  is probably present in the western source.

8 - No emission lines, redshift based on Ca  $H&K$  break.

9 - No lines in the spectra of either members, but there is a clear difference in continuum shapes redward of 4500Å.

10 -  $[OII]$ ,  $H\alpha$ ,  $[NII]$  and Ca  $H&K$  in the eastern object, no lines in the western source.

12 - Strong emission lines:  $[OII]$ ,  $H\alpha$ ,  $[OIII]$  and  $H\beta$  in the western object, no lines in the eastern source.

13 - Eastern object has a narrow emission line at 4904Å, and the western object a broad emission line at 5389Å.

14 - Interacting galaxies based on Keck-II images.

15 - Broad emission feature in the eastern object at 4296Å.

TABLE 1. Lensed Quasar Candidates

#	$\alpha$	$\delta$	<i>Sep</i>	<i>E</i>	<i>O-E</i>		$F^{20cm}$	<i>E</i>	<i>O-E</i>		$F^{20cm}$	$\Delta m_I$	$\Delta m_V$	$\Delta m_B$	$\sigma$	Type & Redshift	
					West	Object			West	Object						West	East
J2000				["]	[mag]	[mag]	[mJy]	[mag]	[mag]	[mag]	[mJy]	[mag]	[mag]	[mag]	[mag]	( <i>T, z</i> )	( <i>T, z</i> )
1	09:11:06.65	+45:43:45.0	22.7	15.6	2.1	6.2	17.3	2.0	1.9	-0.91 ± 0.06	-0.88 ± 0.09	-0.82 ± 0.10	0.7	G,0.098	G,0.099		
2	09:58:58.57	+29:47:53.9	11.4	19.2 <sup>a</sup>	1.3	45.8	19.2	-0.1	138.3	+0.35 ± 0.16	+0.21 ± 0.05	+0.54 ± 0.07	3.2	Q,2.080	Q,2.75?		
3	10:56:10.29	+44:27:16.7	24.5	19.2	0.3	49.5	19.0	0.7	55.0	...	...	...	...	??	Q,?		
4	11:58:44.66	+41:34:26.3	11.7	16.7	1.8	1.1	18.1	2.5	1.0	-1.20 ± 0.12	-1.07 ± 0.11	-1.22 ± 0.08	1.1	G,0.127	G,0.127		
5	12:03:13.79	+24:21:36.3	28.1	18.4 <sup>a</sup>	2.4	17.5	17.2	2.7	3.0	+0.93 ± 0.08	+0.82 ± 0.07	+0.79 ± 0.14	1.0	G,0.229	??		
6	12:06:06.02	+28:55:55.9	8.3	15.5 <sup>a</sup>	3.7	2.7	17.2	3.4	4.0	+0.89 ± 0.06	+0.83 ± 0.09	<sup>b</sup>	0.5	G,0.205	??		
7	12:44:47.77	+31:39:12.0	11.6	17.1	3.1	7.9	17.3	4.0	7.2	-0.24 ± 0.07	-0.35 ± 0.09	-0.68 ± 0.35	1.2	G,0.237	G,0.241		
8	13:04:25.86	+22:38:22.6	28.2	16.5 <sup>a</sup>	3.7	3.4	17.6	2.6	1.6	-0.85 ± 0.04	-0.72 ± 0.03	-0.89 ± 0.09	1.8	G,0.223	G,0.223		
9	13:50:56.42	+50:53:03.6	18.5	19.0	2.7	6.6	17.2	4.4	2.6	+2.30 ± 0.35	+1.87 ± 0.27	+0.62 ± 0.38	3.2	??	??		
10	14:43:56.91	+29:19:16.2	12.6	17.8 <sup>a</sup>	3.1	3.4	16.3	2.9	14.4	+0.50 ± 0.07	+0.54 ± 0.09	+0.51 ± 0.24	0.3	??	G,0.178		
11	14:55:15.47	+30:57:04.4	14.8	17.2 <sup>a</sup>	2.1	4.2	18.2	1.7	1.4	-0.43 ± 0.10	-0.33 ± 0.07	-0.40 ± 0.12	0.7	G,0.158	G,0.159		
12	15:02:08.29	+25:28:44.9	15.9	16.7	1.4	4.1	17.4	2.7	47.1	-1.74 ± 0.09	-1.90 ± 0.09	-2.36 ± 0.16	3.2	G,0.321	G,0.178		
13	16:22:29.54	+35:31:09.1	25.7	19.8	1.7	1.7	19.9	1.7	218.4	...	...	...	...	G,?	Q,?		
14	17:08:03.27	+46:48:59.5	10.1	18.7	1.7	1.7	18.0	1.6	3.3	+0.36 ± 0.06	+0.39 ± 0.08	+0.37 ± 0.09	0.3	G,0.291	G,0.291		
15	17:20:25.47	+48:03:21.4	19.3	19.8	1.0	29.9	19.5	1.0	9.7	...	...	...	...	??	Q,?		

Notes to Table 1.

Double point source radio/optical objects with similar colours (< 3.5 $\sigma$ ). For each pair, the coordinates given in the table are for the western object's radio position. *E* and *O* are the APM *E* and *O* magnitudes, respectively.  $F^{20cm}$  is the integrated radio flux at 20 cm.  $\Delta m_i$  is the measured *i*-band magnitude difference for a pair.  $\sigma$  is defined in Equation 1. (*T, z*) is the type (Q-Quasar; G-Galaxy; ?-Unknown) and redshift of the objects.

<sup>a</sup> - The APM magnitude for at least one band is not known, and therefore the *E* and *O* magnitudes are taken from the USNO-A1.0 catalog. <sup>b</sup> - Close to bright star, difficult to observe in the *B* band.

#### Notes on individual objects:

- 2 - A red spectrum (not shown) of the eastern object shows  $CIII]\lambda 1909$  emission at 7125Å.
- 3 - Unidentified narrow line at 4305Å present only in the western object, and unidentified broad emission feature at 4914Å present only in the eastern object.
- 5 - No lines are present in the spectrum of the eastern object.
- 6 - No emission lines, Ca *H&K* is probably present in the western source.
- 8 - No emission lines, redshift based on Ca *H&K* break.
- 9 - No lines in the spectra of either members, but there is a clear difference in continuum shapes redward of 4500Å.
- 10 - [OII],  $H\alpha$ , [NII] and Ca *H&K* in the eastern object, no lines in the western source.
- 12 - Strong emission lines: [OII],  $H\alpha$ , [OIII] and  $H\beta$  in the western object, no lines in the eastern source.
- 13 - Eastern object has a narrow emission line at 4904Å, and the western object a broad emission line at 5389Å.
- 14 - Interacting galaxies based on Keck-II images.
- 15 - Broad emission feature in the eastern object at 4296Å.